Simulation of DNA damage by photons and ions: effects of DNA conformation, cross sections, and radiation chemistry

Ianik Plante

KBRwyle Science, Technology and Engineering
2400 NASA Parkway, Houston, TX 77058

59th Annual Meeting of the American Association of Physicists in Medicine
Denver, CO
July 31 – August 2, 2017

Heavy ions in space

- **Abundances (a) and Energy Spectrum (b) of GCR**

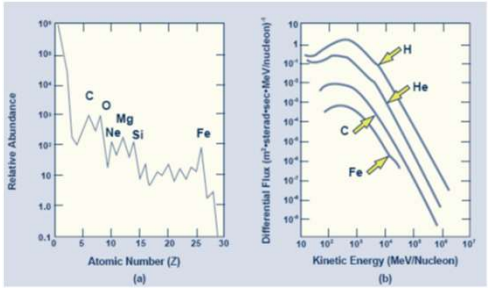

NASA Strategic Plan for Space Radiation Health Research (1998)

The Space Radiation Problem

- **Space radiation is comprised of high-energy protons and heavy ions (HZE's) and secondary protons, neutrons, and heavy ions produced in shielding**
- **Unique damage to biomolecules, cells, and tissues occurs from HZE ions that is qualitatively distinct from X-rays and gamma-rays on Earth**
- **No human data to estimate risk from heavy ions, thus requiring use of biological models and theoretical understanding to assess and mitigate risks**
- **Shielding has excessive costs and will not eliminate galactic cosmic rays (GCR)**

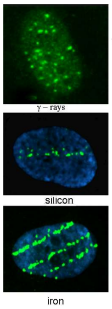

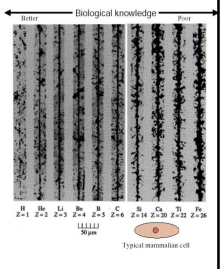

Cucinotta and Durante, Lancet Oncology (2006)

Application of heavy ions to non-NASA environments

- **Heavy ions are used in a few facilities in the world for radiotherapy.**
  - Heavy ions have advantageous energy-deposition profile, allowing them to treat deep tumors and sparing normal tissue
  - The dose can be delivered with a millimeter precision
  - Ions heavier than protons have a higher relative biological effectiveness, and may be more effective to treat otherwise radio-resistant tumors

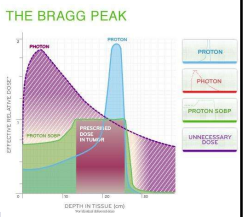

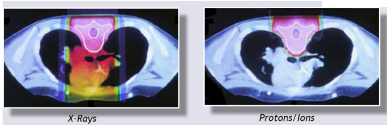

iucf.indiana.edu; ptcri.ox.ac.uk

Multiscale Approach to the Effects of Ionizing Radiation

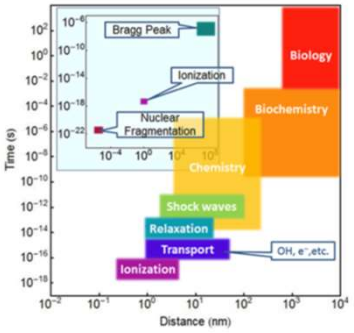

Surdutovich E, Solov'yov AV. *Eur J Phys D* **28**, 353 (2014)

Radiation Track Structure

- **The energy deposition by heavy ions is highly heterogeneous and dependent on the type and energy of the ion**
- **The interaction leads to the formation of radiolytic species such as $H^{\cdot}$, $^{\cdot}OH$, H_2, H_2O_2, e^-_{aq},…**

Primary energy loss events in low-LET tracks

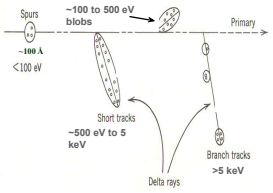

Mozumder A, Magee JL. *Radiat. Res.* **28**, 203 (1966)

Primary energy loss events in high-LET tracks

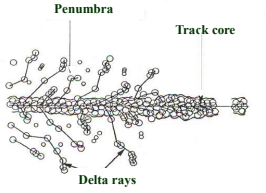

Ferradini C. *J. Chem. Phys.* **76**, 636 (1979)

Particles Transport Basics

- Particles
  - Position (x,y,z)
  - Energy (E)
  - Direction (θ,φ)

$$\vec{v} = \begin{bmatrix} \sin(\theta)\cos(\varphi) \\ \sin(\theta)\sin(\varphi) \\ \cos(\theta) \end{bmatrix}$$

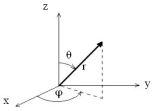

- Cross sections
  - Probability of interaction between radiation and matter

$$dI = -In\sigma dx$$

I: Incident fluence
n: Density of targets
dx: Width
σ: Cross section

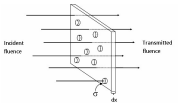

- Cross sections (units: cm^2)
- Mean free path λ (units: cm)

$$I(x) = I(0)\exp(-x/\lambda(E))$$
$$\lambda(E) = 1/(N\sigma(E))$$

Plante I, Cucinotta FA. (2011) Monte-Carlo Simulation of Ionizing Radiation Tracks. In: Mode, C.J. (Ed.) Applications of Monte Carlo Methods in Biology, Medicine and Other Fields of Science. InTech, Rijeka, Croatia. www.intechopen.com

Particles Transport Basics

- Cross sections used in RITRACKS

Ions

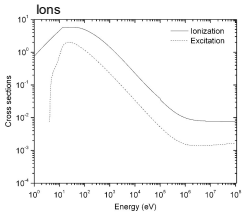

Electrons

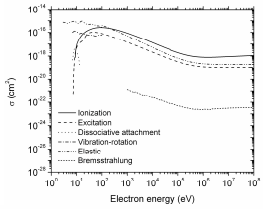

The cross sections for ions are scaled with Z_{eff}:

$$\frac{d\sigma_{ion}(v)}{dW} = Z_{eff}^2 \frac{d\sigma_{proton}(v)}{dW}$$

$$Z_{eff}/Z = 1 - \exp(-125\beta^2/Z^{2/3})$$

v: velocity of the ion
β: relativistic v/c

Plante I, Cucinotta, FA. *New J. Phys.* **11**, 063047 (2009)

Radiation Track Structure

Simulation of $^{1}H^{+}$, $^{12}C^{6+}$, $^{28}Si^{14+}$ and $^{56}Fe^{26+}$ tracks, 100 MeV/amu

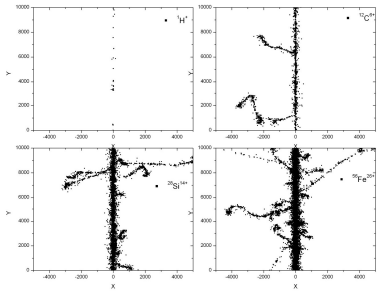

Voxel Dosimetry

Amorphous tracks

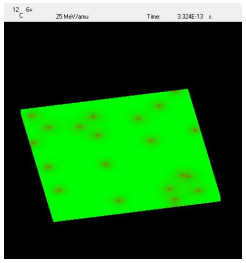

Stochastic tracks

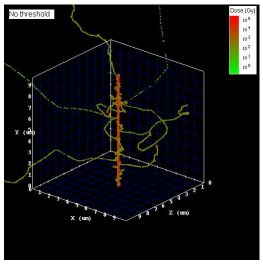

1 GeV/amu $^{56}Fe^{26+}$ ion

LET~150 keV/μm

Voxels: 40 nm × 40 nm × 40 nm

Plante I, et al. *Radiat. Prot. Dosim.* **143**, 156-161 (2011)

Radiation Chemistry

- ~10^{-12} – 10^{-6} s
  - Particles diffusion
  - Chemical reactions

$$G(X) = \frac{\text{Number of chemical species created}}{\text{100 eV deposited energy}}$$

- The radiolytic species are not uniformly distributed, so conventional chemical kinetics models cannot be used.
- An approach based on Green's functions of the diffusion equation (DE) is used.

Examples of chemical reactions:

$e^-_{aq} + e^-_{aq} \xrightarrow{2H_2O} H_2 + 2\,OH^-$

$^\bullet OH + e^-_{aq} \longrightarrow OH^-$

$^\bullet OH + {}^\bullet OH \longrightarrow H_2O_2$

$^\bullet OH + H_2O_2 \longrightarrow HO_2^\bullet + H_2O$

$H^+ + O_2^{\bullet -} \rightleftharpoons HO_2^\bullet$

$H^\bullet + H_2O_2 \longrightarrow {}^\bullet OH + H_2O$

(More than 60 reactions...)

Radiation Chemistry

- Partially diffusion-controlled reaction with rate k_a and reaction radius R

$A + B \xrightarrow{k_a} C$ (Reaction)

$$4\pi R^2 D \left.\frac{\partial p(r,t\,|\,r_0)}{\partial r}\right|_{r=R} = k_a\, p(R,t\,|\,r_0)$$ (Boundary condition)

$$4\pi r r_0 p(r,t\,|\,r_0) = \frac{1}{\sqrt{4\pi Dt}}\left\{\exp\left[-\frac{(r-r_0)^2}{4Dt}\right] + \exp\left[-\frac{(r+r_0-2R)^2}{4Dt}\right]\right\} + \alpha W\left(\frac{r+r_0-2R}{\sqrt{4Dt}}, -\alpha\sqrt{Dt}\right)$$ (Green's function)

$$Q(t\,|\,r_0) = \int_R^\infty 4\pi r^2 p(r,t\,|\,r_0)dr = 1 + \frac{R\alpha+1}{r_0\alpha}\left[W\left(\frac{r_0-R}{\sqrt{4Dt}}, \alpha\sqrt{Dt}\right) - \mathrm{Erfc}\left(\frac{r_0-R}{\sqrt{4Dt}}\right)\right]$$ (Survival probability)

$$\alpha = -\frac{k_a + 4\pi RD}{4\pi R^2 D}$$

The probability of reaction $P(t|r_0) = 1 - Q(t|r_0)$. At each time step, the probability of reaction is assessed. If the particles have not reacted, their relative distance is obtained by sampling the Green's function using the algorithm described in Plante et al. (2013).

Plante I, et al. *J. Comput. Phys.* **242**, 531-543 (2013)

Radiation chemistry

- The independent reaction times (IRT) method
- Used to determine the time evolution of the yields without calculating the positions of the species
- The ultimate probability of reaction of a pair is

$$W_\infty = \frac{1+R\alpha}{r_0\alpha}$$

- The reaction times are determined by solving the equation numerically for t, given a random number U

$$\frac{R\alpha+1}{r_0\alpha}\left[W\left(\frac{r_0-R}{\sqrt{4Dt}},\alpha\sqrt{Dt}\right)-Erfc\left(\frac{r_0-R}{\sqrt{4Dt}}\right)\right]=U$$

- The reaction times are sorted, and the pairs of particles with the shortest reaction times react first

Green's Function for Radiation Chemistry

- Simple case: partially diffusion-controlled reaction with rate k_a and reaction radius R

$$A + B \xrightarrow{k_a} C$$

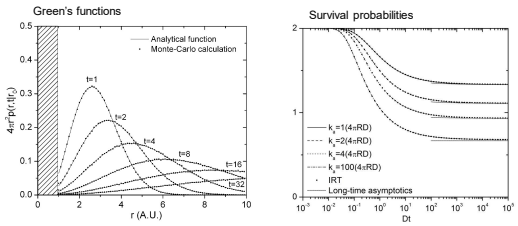

Plante I, et al. *J. Comput. Phys.* **242**, 531-543 (2013)

Radiation Chemistry

Simulation of the time evolution of a $^{12}C^{6+}$ track, 100 MeV/u

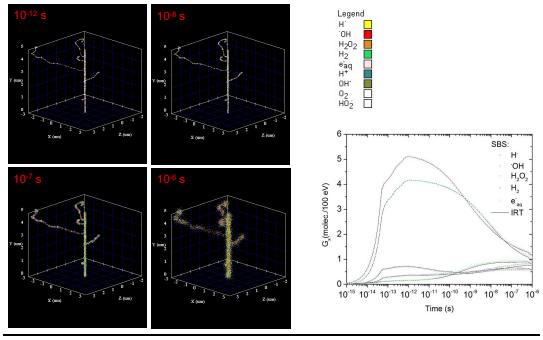

Radiation Chemistry

Simulation of the time evolution of a $^{12}C^{6+}$ track, 100 MeV/u

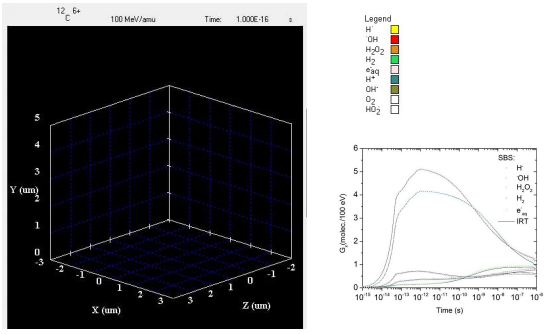

Radiation chemistry and biochemical networks

- There is a growing interest for modeling complex biochemical networks and metabolic pathways
- Most of these pathways can be broken down into enzymatic reactions
- Enzymatic reactions can be described by conventional reaction kinetics
- What is the link with the Green's function approach ?

Example of biochemical network: TGFβ pathway

Model of the system

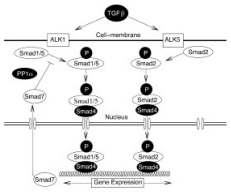

A set of coupled differential equations

$$\frac{d[T1R_{Surf}]}{dt} = \gamma_{T1R} - k_{1Conv}[T1R_{Surf}] + k_{rConv}[T1R_{Conv}] - k_{1Ext}[T1R_{Surf}] + k_{rExt}[T1R_{Ext}] + k_{rConv}[LRC_{Conv}] - k_{LRC}[TGF\beta][T1R_{Surf}][T2R_{Surf}] \quad (1)$$

$$\frac{d[T1R_{Conv}]}{dt} = k_{1Conv}[T1R_{Surf}] - k_{rConv}[T1R_{Conv}] \quad (2)$$

$$\frac{d[T1R_{Ext}]}{dt} = k_{1Ext}[T1R_{Surf}] - k_{rExt}[T1R_{Ext}] - k_{deg}^{T1R}[T1R_{Ext}] \quad (3)$$

Typical solution

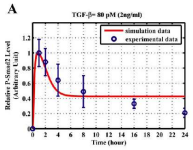

Melke, P. (2006), *Biophys. J.* **91**, 4368-4380; Zi, Z and Klipp, E. (2007), *PLoS ONE* **2**, e936

First and second order reaction kinetics

Reaction
$A \rightarrow B$ or $A \rightarrow B + C$

Rate law
$v = kA$

Mass action law
$\frac{dA}{dt} = -kA \qquad A(t) = A_0 e^{-kt}$

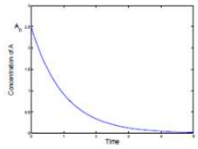

Reaction
$2A \rightarrow B$ or $2A \rightarrow B + C$

Rate law
$v = kA^2$

Mass action law
$\frac{dA}{dt} = -2kA^2 \qquad A(t) = \frac{A_0}{1 + 2A_0kt}$

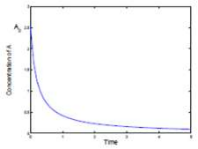

The Green's functions approach used for radiation chemistry is not in agreement with this theory!

Gonze D and Kaufman M. Chemical and enzyme kinetics.

Simulation of chemical reactions

❑ **Boundary conditions**

No boundary (Infinite)

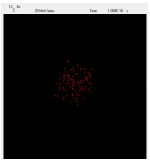

Periodic boundary conditions

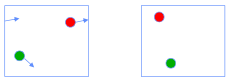

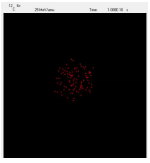

Reaction kinetics

❑ **The distribution of distances in a box is given by**

$$p_{dist}(l) = \begin{cases} -l^2[(l-8)l^2 + \pi(6l-4)] & 0 \le l \le 1 \\ 2l\left[\left(l^2 - 8\sqrt{l^2-1} + 3\right)l^2 - 4\sqrt{l^2-1} + 12l^2\sec^{-1}l + \pi(3-4l) - 1/2\right] & 1 < l \le \sqrt{2} \\ l(1+l^2)\left(6\pi + 8\sqrt{l^2-2} - 5 - l^2\right) - 16l^2\csc^{-1}\sqrt{2 - \frac{2}{l^2}} + 16l^2\tan^{-1}\left(l\sqrt{l^2-1}\right) - 24l(l^2+1)\tan^{-1}\sqrt{l^2-2} & \sqrt{2} < l \le \sqrt{3} \end{cases}$$

❑ **Therefore, the probability of a H· and a ·OH randomly placed in the box to survive up to time t is given by**

$$Q_{box}(t) = \int_{\sigma}^{\sqrt{3}L} Q_{II}(t|l)p_{dist}(l)dl$$

$$Q_{II}(t|r_0) = 1 - \frac{\sigma\alpha + 1}{r_0\alpha}\left[Erfc\left(\frac{r_0 - \sigma}{\sqrt{4Dt}}\right) - W\left(\frac{r_0 - \sigma}{\sqrt{4Dt}}, -\alpha\sqrt{Dt}\right)\right]$$

http://mathworld.wolfram.com/CubeLinePicking.html

Reaction kinetics

- **By using the PBC and sufficiently small time steps, the classical reaction kinetics can be obtained using the Green's functions**

First order kinetics

$$[A] = [A]_0 e^{-k_a [\theta] t}$$

Second order kinetics

$$[A] = \frac{[A]_0}{1 + 2k_a t}$$

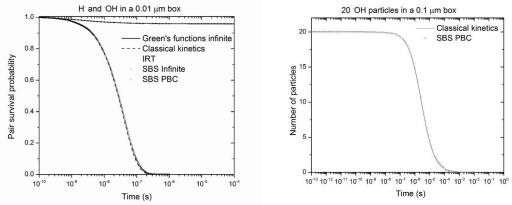

Plante I, Devroye L. Radiat. Phys. Chem. 139, 157-152 (2017).

Discussion

- **The conventional approach is to write down macroscopic rate equations and solve the corresponding differential equations**
  - It is assumed that the concentrations are large and that fluctuations can be neglected
  - Fluctuations are added by introducing a noise term in the macroscopic rate equation
  - The particles are assumed to be uniformly distributed
- **With the Green's function approach**
  - This method is fully stochastic and able to simulate very low concentrations of particles
  - The approach works in two simple cases. We hope to apply this approach to more complex systems, notably enzymes

DNA Damage Simulations

- To better understand DNA damage, several DNA models were implemented in RITRACKS
- The chromatin fiber is build from nucleosome units and linker DNA
- Chromosomes are simulated by random walk, with domain constraints

Linear DNA fragment | Nucleosome | Chromatin fiber | Nuclei

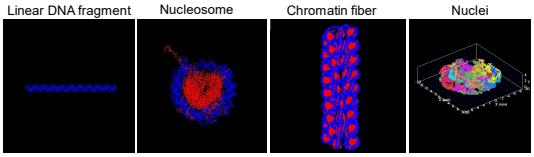

Nuclei simulations courtesy of Artem Ponomarev, PhD

DNA Damage Simulations

- In the DNA bases, there are many internal and valence electrons. The BEB model allows to model the ionization for each electron of the molecule.

Thymine

	No	U (eV)	B (eV)	N
Internal electrons (18)	1	794.1	559.41	2
	2	794.1	559.18	2
	3	601.5	425.6	2
	4	601.5	425.48	2
	5	435.9	311.36	2
	6	435.9	310.41	2
	7	435.8	308	2
	8	435.7	306.41	2
	9	435.8	305.8	2
Valence electrons (44)	10	66.26	40.06	2
	11	71.74	39.14	2.04
	12	63.05	36.16	1.86
	13	57.89	34.56	1.85
	14	44.95	30	2.3
	15	43.96	26.22	2.35
	16	47.64	25.14	2.11
	17	40.64	24.85	2.15
	18	41.92	21.32	2.18
	19	39.28	20.94	2.02
	20	36.32	19.4	1.86
	21	44.53	18.7	2.05
	22	55.89	18.56	1.92
	23	54.72	17.59	1.99
	24	39.88	16.62	2.01
	25	46.93	16.15	2.03
	26	39.89	15.44	1.78
	27	47.3	13.96	1.83
	28	59.96	13.15	1.86
	29	54.12	12.31	2.07
	30	60.23	12.10	1.78
	31	40.38	9.27	1.97

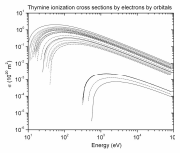

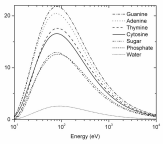

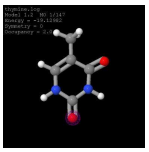

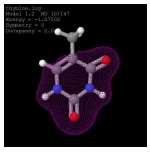

Calculations of MO from the site www.chemeddl.org

DNA Damage Simulations

- In addition to ionization, it is now well established that low-energy electrons can damage DNA, including DSB
- Mechanism: dissociative attachment to resonant states

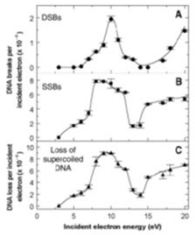

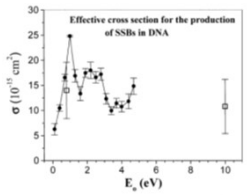

Boudaïffa B, et al. *Science* **287**, 1658 (2000); Panajotovic R, et al. *Radiat. Res.* **165**, 452-459 (2006)

DNA Damage Simulations

- **Cross sections can be calculated for the bases, sugars and phosphates.**
- **In this case, the medium is considered a succession of homogeneous media.**

$$dI = -IN\sigma dx$$

$$\ln(I/I_0) = -\int_0^x \sigma(u)\,N\,du$$

$$I = I_0 \exp\left\{-N\left[\sum_{j=1}^{i-1}(\sigma_j - \sigma_i)W_j + \sigma_i x\right]\right\}$$

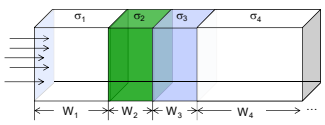

Relative weight

$$p_i = I_0 \frac{\exp(-N\sum_{j=1}^{i-1} W_j\sigma_j)(1-\exp(-NW_i\sigma_i))}{N\sigma_i}$$

Sampling of W_s

$$W_s = \sum_{j=1}^{i-1} W_j - \frac{1}{N\sigma_i}\log[1 - V(1 - e^{-\sigma_i NW_i})]$$

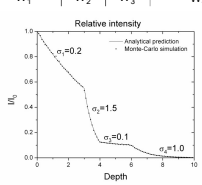

Adapted from S. Edel, PhD Dissertation, Université de Toulouse (2006)

Radiation Chemistry (DNA)

- The radiation chemistry of DNA is very complex
- Many reaction rate constants are known

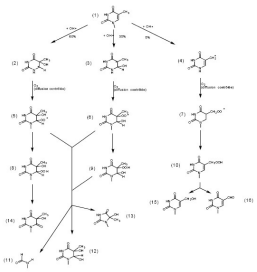

Reaction	k ($dm^3.mol^{-1}.s^{-1}$)	Radius (Å)
e^-_{aq}+Thymine→Thy(+e)	$1.79x10^{10}$	5.287
·OH + Thymine → TC5OH+TC6OH+TUCH2·	$6.4x10^9$	3.02
H.+Thymine→Thymine*	$5.7x10^8$	0.11

Cadet J, et al. *Reviews in Physiology, Biochemistry and Pharmacology* **31**, 1-87 (1997)

DNA Damage Simulations

- Classification of DNA damage

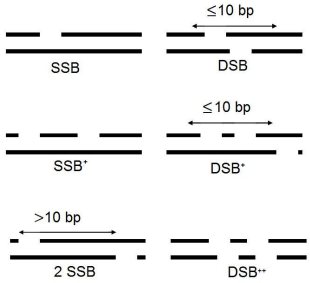

Adapted from S. Edel, PhD Dissertation, Université de Toulouse (2006)

DNA damage simulations

- **Formation of complex damage in linear DNA**

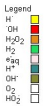

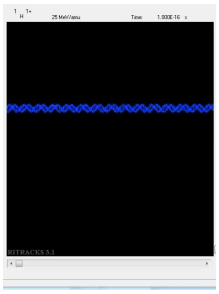

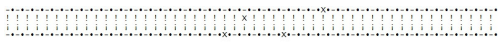

DNA damage simulations

- Initial yields calculations with protons

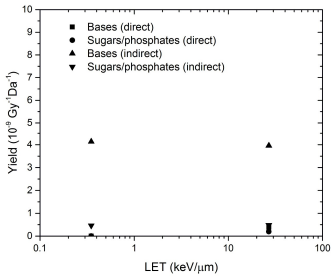

DNA damage simulations

- Chromatin fiber
- For this simulation
  - 7 sites damaged by direct effect
  - 36 sites damaged by indirect effect
- No histones proteins included

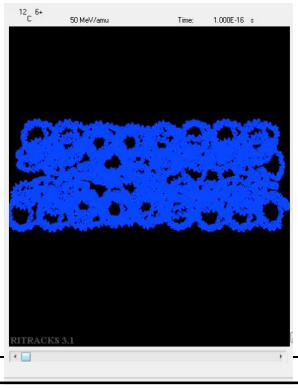

Histones

- Proteins used to package DNA in nucleosomes and chromatin fiber
- Nucleosome: 8 histone proteins
- About 147 base pairs of DNA
- Histones might play roles in DNA repair
- These proteins are composed by amino acids, for which cross sections and reaction rate constants are known
- Therefore the approach used for DNA damage can also be used for histone damage and is now included in RITRACKS

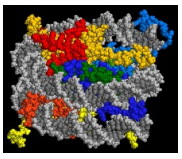

Histones H2A, H2B, H3 and H4 are colored, DNA is gray.

From https://en.wikipedia.org/wiki/Nucleosome

DNA damage simulations

- With histones

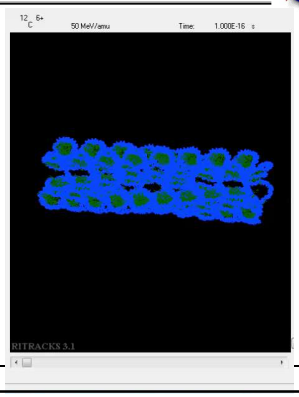

DNA Damage / γH2AX Foci Studies

- Irradiation by 1 GeV/amu Fe ions
- 100 cGy
- LET ~ 148 keV/μm

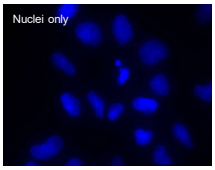

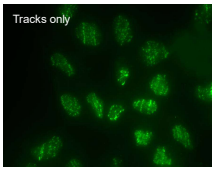

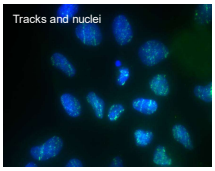

Experiments performed at the NASA Space Radiation Laboratory (2007)

DNA damage / γH2AX foci studies

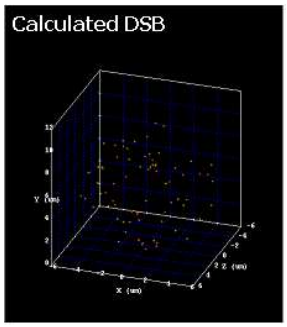

2700 x $^{1}H^{+}$, 300 MeV (1 Gy)
Dose in voxels (20 nm)
Chromosomes (Random Walk model)
Intersection voxels
H2AX foci experiments

The probability of at least on

$\psi = 1 - e^{-QD(1)}$ DSB at a voxel

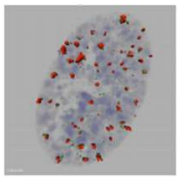

Mukherjee, B. et al. (2008), *DNA repair* **7** 1717-1730; Plante, I. et al. (2013), *Phys. Med. Biol.* ***58****, 6393-6405*

DNA damage / γH2AX foci studies

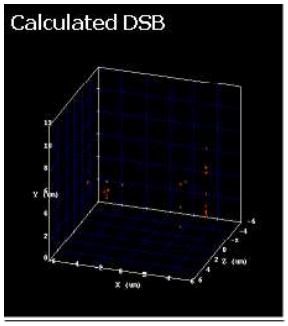

6 x $^{56}Fe^{26+}$, 1 GeV/u (1 Gy)
Dose in voxels (20 nm)
Chromosomes (RW model)
Intersection voxels
H2AX foci experiments

The probability of at least one DSB at a voxel

$$\psi = 1 - e^{-QD(t)}$$

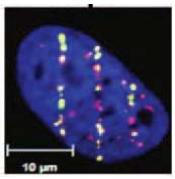

Asaithamby, A. et al. (2008) *Radiat. Res.* **169**, 437-446; Plante, I. et al. (2013), *Phys. Med. Biol.* ***58****, 6393-6405*

DNA Damage / γH2AX Foci Studies

- Calculation of DSBs by $^{1}H^{+}$, $^{12}C^{6+}$ and $^{56}Fe^{26+}$ ions

Simulation results

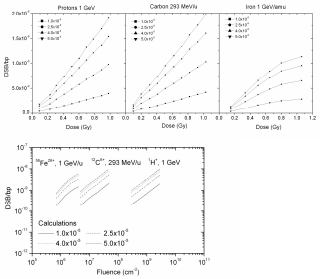

Compare with

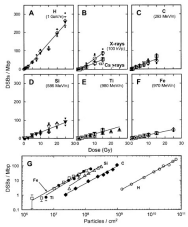

=> Several orders of magnitude of difference but similar trend!

Plante I, et al. *Phys. Med. Biol.* **58**, 6393-6405 (2013); Hada M, Sutherland B. *Radiat. Res.* **165**, 223-230 (2006)

DNA Damage / γH2AX Foci Studies

- **Superresolution microscopy**
  - Shows nanostructure of carbon ion radiation-induced DNA double-strand break repair foci
  - The organization of the subfoci suggests that they could represent the local chromatin structure of elementary DSB repair units at the DSB damage sites
  - 1 foci ≡ 1 DSB ?? Subfoci seems to represent individual nucleosomes containing γ-H2AX

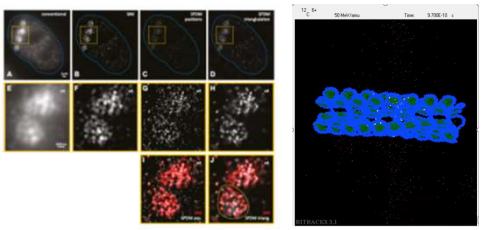

Lopez Perez R. et al. *FASEB.* **30**, 2767-2776 (2016)

Chromosome Aberrations

- Damaged DNA may be repaired improperly, leading to various types of chromosome aberrations
- Chromosome aberrations are linked to cancer and can be used as a biomarker for cancer risk associated with radiation exposure
- Some ions are more efficient for the creation of chromosome aberrations

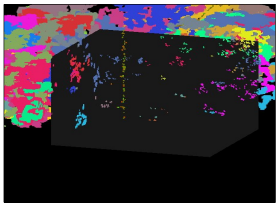

Simulation of chromosomes by random walk and the track of a $^{12}C^{6+}$ ion, 25 MeV/n

The slicer illustrates how chromosomes are in proximity

Chromosome aberrations

- **Simulations: the nucleus is put in an irradiated volume, which is a box of adjustable dimensions**
- **The number of tracks are chosen such that the dose corresponds to the requested dose**
- **periodic boundary conditions: the delta-rays that escape the volume are put back on the opposite side**

Clip tracks that go outside the volume

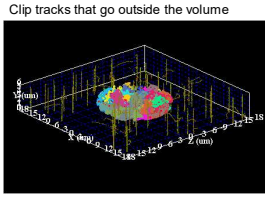

Periodic boundary conditions

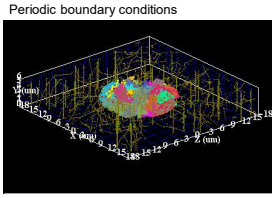

Irradiation of a volume, 36 μm x 36 μm x 6 μm, using $^{12}C^{6+}$, 25 MeV/n. Dose: 0.1 Gy

Ponomarev A.L. et al., submitted.

Chromosome aberrations types calculated in the BDSTracks code

- **Deletions**

- **Interchromosomal translocations**

- **Dicentrics**

- **Terminal deletions**

- **Intrachromosomal translocations**

- **Rings**

- **Paracentric inversions**

- **Interchromosomal insertions**

- **Pericentric inversions**

- **Complex exchanges**

Chromosome aberrations

- Simulation with BDSTracks (Biological Damage by Stochastic Tracks)
- Calculated dose-response curves and comparison with experimental data

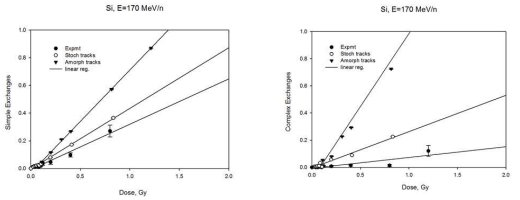

Ponomarev A.L. et al., submitted.

Chromosome aberrations

- Deletions

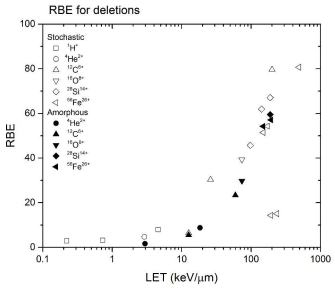

Ponomarev et al., submitted.

Chromosome aberrations

- Exchanges

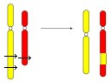

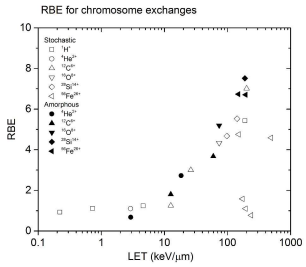

Ponomarev et al., submitted.

Cells and Tissue Models

- Many tissue and cell culture models are based on Voronoi tessellation (in 2D and 3D)
- A Voronoi cell is the space closest to a given point (than the other points)
- Models derived from microscopic images can also be used

A 2D voronoi cell

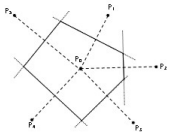

Simulation of a 2D cell culture using a simple Voronoi cell tessellation and clipping

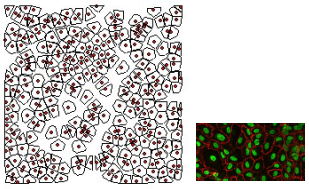

http://www.elveflow.com/wp-content/uploads/2014/05/Endothelial-cell-culture-laminar-flow-perfusion.jpg

Tissue Models

- Voronoi cell tessellation in 3D was included in RITRACKS
- Multi-scale modelling

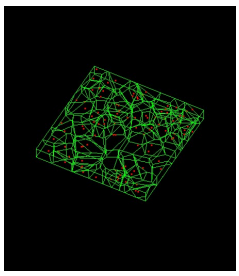

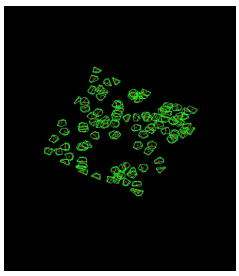

Tissue Models

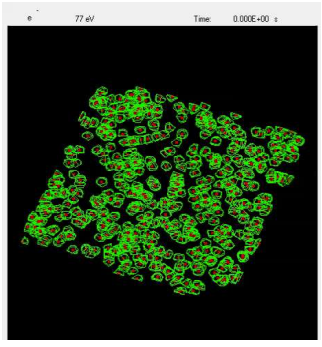

Algorithm to Determine if a Point is Inside a Cell

- Typical Voronoi-like 3D cell

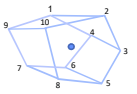

Face	Vertices (in order)
I	1,2,3,4
II	1,9,10,2
III	7,8,10,9
IV	8,7,6,5
V	5,6,4,3
VI	10,8,5,3,2
VII	1,4,6,7,9

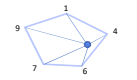

Polyhedron face VII

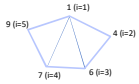

Decomposition of face into triangles

Vertices (1,i+k,i+k+1), k=1,N-2

Works for convex figures only!!

Calculation of solid angle (Ω) for each triangle pyramid using L'Huilier's theorem

$$\cos\theta_a = \frac{\overline{OB}\cdot\overline{OC}}{\|\overline{OB}\|\|\overline{OC}\|}$$

$$\cos\theta_b = \frac{\overline{OA}\cdot\overline{OC}}{\|\overline{OA}\|\|\overline{OC}\|}$$

$$\cos\theta_c = \frac{\overline{OA}\cdot\overline{OB}}{\|\overline{OA}\|\|\overline{OB}\|}$$

$$\theta_s = \frac{\theta_a + \theta_b + \theta_c}{2}$$

$$\tan\left(\frac{\Omega}{4}\right) = \sqrt{\tan\left(\frac{\theta_s}{2}\right)\tan\left(\frac{\theta_s-\theta_a}{2}\right)\tan\left(\frac{\theta_s-\theta_b}{2}\right)\tan\left(\frac{\theta_s-\theta_c}{2}\right)}$$

The point is inside the cell if the sum of all solid angles of all triangles of all faces is 4π.

Similarly, the volume of the cell is obtained by summing the volume of all pyramid, using

$$V = \frac{1}{6}\|\overline{OA}\times\overline{OB}\cdot\overline{OC}\|$$

Algorithm to Determine if a Point is Inside a Cell

- Use with RITRACKS visualization interface
- The algorithm seems to work fine for the case studied
- Since the calculation of the volume can be done similarly, dose can be calculated in cells

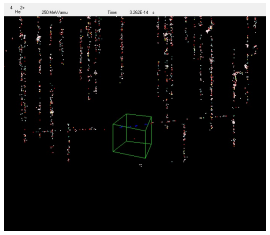

Comments:

- The algorithm is rather slow. A screening algorithm determine first if the point is inside a sphere encompassing the cell.
- The algorithm is not expected to work for non-convex cells in its actual form.
- The argument inside the square root in L'Huilier's equation is occasionally negative. This problem was solved by taking the absolute value. However it is not clear that doing this is justified and how this affects the algorithm

Future Development Plans

- Predictions of clustered and complex DNA damage yields in human cells for improving the understanding of DNA repair and signal transduction
- Add the low-energy electron cross sections and other DNA damage mechanisms
- Add histone cross sections and reactions for simulation of DNA damage to the chromatin fiber
- Use with chromosome models to study double-strand breaks (DSB) and chromosome aberrations in relation to cancer risks from space radiation
- Links with "Omics" to determine gene and pathways affected by DNA damage and chromosome aberrations
- Tissue models

Acknowledgements

- KBRwyle
  - Artem Ponomarev
  - Shaowen Hu
  - Kerry George
- Lockheed Martin
  - Cliff Amberboy
- NASA JSC
  - Honglu Wu
- NASA Langley
  - Steve Blattnig
- McGill University
  - Luc Devroye

References

- Plante I, Ponomarev AL and Cucinotta FA (2011). Radiat. Prot. Dosim., 143, 156-161.
- Plante I and Cucinotta FA (2011). Book chapter published in: Mode, CJ (Ed.) Applications of Monte-Carlo Methods in Biology, Medicine and Other fields of Science. InTech, Rijeka, Croatia.
- Durante M, and Cucinotta FA (2011), The Physical Basis for Radiation Protection in Space. Reviews of Modern Physics 83, 1245-1281.
- Plante I and Cucinotta FA (2010). Radiat. Env. Biophys. 49, 5-13.
- Plante I and Cucinotta FA (2008). New J Phys 10, 125020.
- Plante I and Cucinotta FA (2009). New J Phys 11, 063047.
- Cucinotta FA, and Durante M (2006). Cancer risk from exposure to galactic cosmic rays: implications for space exploration by human beingsThe Lancet Oncology 7, 431-435.
- Cucinotta FA, Nikjoo H, and Goodhead DT (2000). Model of The Radial Distribution of Energy Imparted in Nanometer Volumes From HZE Particle. Radiat Res 153, 459-468.
- Cucinotta FA, Nikjoo H, and Goodhead DT (1999), Applications of Amorphous Track Models in Radiobiology. Radiat Environ Biophys 38, 81-92.
- Cucinotta FA, Katz R, and Wilson JW (1998), Radial Distributions of Electron Spectra from High-Energy Ions. Radiat Environ Biophys 37, 259-265.